

Energy-momentum tensor correlators and spectral functions

Harvey B. Meyer

*Center for Theoretical Physics, Massachusetts Institute of Technology,
Cambridge, MA 02139, U.S.A.*

E-mail: meyerh@mit.edu

ABSTRACT: We calculate the thermal Euclidean correlators and the spectral functions of the energy-momentum tensor for pure gauge theories, including at non-zero spatial momentum, at leading order in perturbation theory. Our goal is to improve the extraction of transport properties from Euclidean correlators that are computable in lattice QCD. Based on our results and the predictions of hydrodynamics for the structure of the spectral functions at low frequencies, we show that the shear and bulk viscosities can advantageously be extracted from the Euclidean correlators of the conserved charges, energy and momentum, at small but non-vanishing spatial momentum. The spectral functions in these channels are free of the ultraviolet ω^4 term which represents a large background to the thermal physics encoded in the correlators of the fluxes.

KEYWORDS: Lattice QCD, Thermal Field Theory.

Contents

1. Introduction	1
2. Perturbative calculation	3
2.1 Zero temperature	4
2.2 Finite temperature	5
2.2.1 Finite momentum	5
3. Physics discussion	6
A. Calculation of Euclidean correlators	8
A.1 The $\langle T_{12}(0) T_{12}(x) \rangle$ correlator	8
A.2 $\langle T_{11} T_{11} \rangle$ with momentum along x direction	11
A.3 Scalar correlator with non-zero momentum	11
B. Calculation of spectral functions	12
C. The spectral function in terms of polylogarithms	13

1. Introduction

The particles produced in RHIC heavy-ion collisions exhibit sizeable elliptic and radial flow [1–4]. This is a signature of collective behavior, which the equations of ideal hydrodynamics have been able to describe quite successfully [5–7]. The leading corrections in a gradient expansion of flow velocities is parametrized by shear and bulk viscosity, η and ζ . Detailed viscous relativistic hydrodynamics calculations [8–13] find that the experimental data excludes a shear viscosity to entropy density ratio larger than about 0.3, in agreement with early rough estimates [14]. This would make the substance created an exceptionally good fluid [15], and it is therefore of primary interest to improve our knowledge of the transport coefficients of the quark-gluon plasma.

Theoretically, the transport coefficients can be extracted from the imaginary part of a retarded two-point correlation function; this imaginary part is called the spectral function and is denoted by $\rho(\omega)$. This is the content of the Kubo formulas [16]. By analytic continuation, the spectral function is also related to Euclidean correlators C_E [17, 18], which are functions of Euclidean time x_0 , spatial momentum \mathbf{q} and temperature T , by

$$C_E(x_0, \mathbf{q}, T) = \int_0^\infty d\omega \rho(\omega, \mathbf{q}, T) \frac{\cosh \omega(x_0 - \frac{1}{2T})}{\sinh \frac{\omega}{2T}}. \quad (1.1)$$

The spectral functions are odd in ω and have everywhere the same sign as ω . Since viscosities parametrize the dissipation of momentum, the relevant operators are elements of the energy-momentum tensor $T_{\mu\nu}$. Because the temperatures reached at RHIC are not much larger than twice the critical temperature T_c where a gas of hadrons rapidly crosses over to a system with many more degrees of freedom (see [19] and ref. therein), perturbative methods [20–24] are not directly applicable. They can however tell us about the asymptotic high T behavior of the viscosities and the associated spectral functions. They also allow us to familiarize ourselves with the intricate kinematics that arise at non-zero temperature and spatial momentum, one of the objectives of this work. Finite-momentum meson spectral functions were investigated analytically in [25].

Lattice calculations of viscosities [26–28, 17] have so far mostly focused on the Euclidean correlators of T_{12} for the shear viscosity, and T_{ii} (or $T_{\mu\mu}$) for the bulk viscosity. Indeed the Kubo formulas read in these cases

$$\eta(T) = \pi \lim_{\omega \rightarrow 0} \frac{\rho_{12,12}(\omega, \mathbf{0}, T)}{\omega}, \tag{1.2}$$

$$\zeta(T) = \frac{\pi}{9} \lim_{\omega \rightarrow 0} \frac{\rho_{ii,jj}(\omega, \mathbf{0}, T)}{\omega}, \tag{1.3}$$

where $\rho_{\mu\nu,\rho\sigma}$ corresponds to $\langle T_{\mu\nu} T_{\rho\sigma} \rangle$. As we shall review in section 3, hydrodynamics, as an effective theory describing low-frequency phenomena around equilibrium, predicts the functional form of the spectral functions in these channels, including at small but non-vanishing \mathbf{q} .

Leaving aside the problem of determining the spectral function given the Euclidean correlator, a particular difficulty in this approach is that the spectral functions grow as ω^4 (times a power series in α_s) at large frequencies. This buries the contribution from the small ω region under a much larger contribution (by a factor of at least five) from ultraviolet modes. The latter contribution is almost temperature independent and therefore does not advance in any way our understanding of thermal physics. Given that the Euclidean correlators are determined by Monte-Carlo methods and carry statistical errors, this is a significant drawback. The difficulty is far more severe than in studies of the charmonium spectral functions [29–31], or calculations of the electromagnetic conductivity [32], because the spectral function only grows as ω^2 for the vector current $\bar{\psi}\gamma_i\psi$.

Methods to subtract the ultraviolet contribution to the Euclidean correlator, and hence to enhance the sensitivity of the lattice observables to the low-frequency region described by hydrodynamics, have been proposed and implemented [18]. One of these methods (subtracting the $T = 0$ spectral function) has the virtue of removing the ω^4 contribution completely, by contrast with a perturbative order-by-order subtraction. The drawback is that positivity of the integrand in eq. (1.1) is given up, and a large part of the signal is lost in the difference, an unfavorable situation from the numerical point of view.

Here, based on the exact Ward identities that follow from the conservation of the energy-momentum tensor, we show that the spectral function of the energy density operator with non-vanishing spatial momentum goes to a constant as $\omega \rightarrow \infty$. Similarly, the two-point function of the momentum density operator grows only as ω^2 . This is confirmed by

our perturbative calculation. These Euclidean correlators are therefore far more sensitive to the thermal effects than the correlators of the fluxes. Yet provided \mathbf{q} is sufficiently small, their low-frequency region is still described by hydrodynamics, and therefore the shear and bulk viscosity can be extracted from them.

We collect leading perturbative results on the Euclidean correlators and spectral functions in section 2, and discuss in section 3 the interplay of the perturbative predictions with the hydrodynamics predictions to propose a new way to extract shear and bulk viscosity from Euclidean correlators.

2. Perturbative calculation

The Euclidean energy-momentum tensor for $SU(N_c)$ gauge theories reads

$$T_{\mu\nu}(x) = \theta_{\mu\nu}(x) + \frac{1}{4}\delta_{\mu\nu}\theta(x) \quad (2.1)$$

$$\theta_{\mu\nu}(x) = \frac{1}{4}\delta_{\mu\nu}F_{\rho\sigma}^a F_{\rho\sigma}^a - F_{\mu\alpha}^a F_{\nu\alpha}^a \quad (2.2)$$

$$\theta(x) = \frac{\beta(g)}{2g} F_{\rho\sigma}^a F_{\rho\sigma}^a \quad (2.3)$$

$$\beta(g) = -b_0 g^3 + \dots, \quad b_0 = \frac{11N_c}{3(4\pi)^2}. \quad (2.4)$$

In the U(1) case, the summation over the adjoint index a is trivial and of course $\beta(g) = 0$. In contrast with Minkovsky space, $T_{0i} = \theta_{0i}$ is an antihermitian operator. In particular, $\langle T_{0i}(x)T_{0i}(0) \rangle < 0$ for $x \neq 0$, and $P_j = i \int d^3\mathbf{x} T_{0j}(x)$ is the usual momentum operator, for instance $P_j|\mathbf{q}\rangle = q_j|\mathbf{q}\rangle$ for a one-particle state.

In view of the form of the energy-momentum tensor, we consider now the connected correlators of the field strength tensor and those of the field strength tensor squared, at leading order in perturbation theory. The expectation values obtained in that approximation are denoted by $\langle \dots \rangle_0$ and throughout this paper we keep only connected diagrams. The effect on spectral functions of using Hard-Thermal Loop resummed perturbation theory [33] in the region $\omega < T$ is beyond the scope of this work. Nevertheless our results are perfectly physical, since they are exact in the U(1) case.

In Feynman gauge, we have

$$\langle F_{\mu\nu}(x)F_{\alpha\beta}(y) \rangle_0 = d_A \phi_{\mu\nu\alpha\beta}(x-y), \quad (2.5)$$

$$\phi_{\mu\nu\alpha\beta}(x) \equiv \delta_{\nu\beta}f_{\mu\alpha}(x) + \delta_{\mu\alpha}f_{\nu\beta}(x) - \delta_{\mu\beta}f_{\nu\alpha}(x) - \delta_{\nu\alpha}f_{\mu\beta}(x), \quad (2.6)$$

$$f_{\mu\alpha}(x) \equiv T \sum_{p_0} \int \frac{d^3\mathbf{p}}{(2\pi)^3} \frac{e^{i(p_0 x_0 + \mathbf{p}\cdot\mathbf{x})}}{p_0^2 + \mathbf{p}^2} p_\alpha p_\mu. \quad (2.7)$$

One then easily obtains

$$\langle F_{\mu\nu}^a(x)F_{\rho\sigma}^a(x)F_{\alpha\beta}^b(y)F_{\gamma\delta}^b(y) \rangle_0 = d_A \left[\phi_{\mu\nu\alpha\beta}(x-y)\phi_{\rho\sigma\gamma\delta}(x-y) + \phi_{\mu\nu\gamma\delta}(x-y)\phi_{\rho\sigma\alpha\beta}(x-y) \right]. \quad (2.8)$$

The color factor is $d_A \equiv N_c^2 - 1$ for $SU(N_c)$ and 1 for $U(1)$. To study mixed correlators (which are functions of (x_0, \mathbf{p})), we introduce the spatial Fourier transform of $\phi_{\mu\nu\alpha\beta}(x)$, $\tilde{\phi}_{\mu\nu\alpha\beta}(\mathbf{p}, x_0) = \int d^3\mathbf{x} \phi_{\mu\nu\alpha\beta}(x) e^{i\mathbf{p}\cdot\mathbf{x}}$. Then

$$\begin{aligned} & \int d^3\mathbf{y} e^{i\mathbf{q}\cdot\mathbf{y}} \langle F_{\mu\nu}^a(0) F_{\rho\sigma}^a(0) F_{\alpha\beta}^b(x_0, \mathbf{y}) F_{\gamma\delta}^b(x_0, \mathbf{y}) \rangle_0 \\ &= d_A \int \frac{d^3\mathbf{p}}{(2\pi)^3} \left[\tilde{\phi}_{\mu\nu\alpha\beta}(\mathbf{p}, x_0) \tilde{\phi}_{\rho\sigma\gamma\delta}(-(\mathbf{p}+\mathbf{q}), x_0) + \tilde{\phi}_{\mu\nu\gamma\delta}(\mathbf{p}, x_0) \tilde{\phi}_{\rho\sigma\alpha\beta}(-(\mathbf{p}+\mathbf{q}), x_0) \right]. \end{aligned} \quad (2.9)$$

The integral is worked out in appendix A. The results are of course gauge-invariant. In the next two subsections, we present the results in a number of channels of physical interest. Throughout this section, we align the spatial momentum with the z -axis, $\mathbf{q} = q\hat{e}_3$, $q \geq 0$. Since the spectral function is odd in ω , we also choose $\omega \geq 0$ without loss of generality. The most general results are given at the end of the section, however we find it useful to give the explicit form in the simpler cases of zero temperature or zero momentum.

2.1 Zero temperature

At $T = 0$ and zero spatial momentum, by dimensional analysis, the correlation functions at tree-level all fall off as $1/x_0^5$. With finite-momentum and for $x_0 > 0$,

$$\int d^3\mathbf{x} e^{i\mathbf{q}\cdot\mathbf{x}} \langle T_{13}(x) T_{13}(0) \rangle_0 = \frac{d_A e^{-qx_0}}{5(4\pi)^2 x_0^5} (qx_0 + 2)(q^2 x_0^2 + 3qx_0 + 6), \quad (2.10)$$

$$\rho_{13,13}(\omega, q) = \frac{d_A \theta(\omega - q)}{10(4\pi)^2} \omega^2 (\omega^2 - q^2), \quad (2.11)$$

$$\int d^3\mathbf{x} e^{i\mathbf{q}\cdot\mathbf{x}} \langle T_{12}(x) T_{12}(0) \rangle_0 = \frac{4d_A e^{-qx_0}}{5(4\pi)^2 x_0^5} (3 + qx_0 + q^2 x_0^2) \quad (2.12)$$

$$\rho_{12,12}(\omega, q) = \frac{d_A \theta(\omega - q)}{10(4\pi)^2} (\omega^2 - q^2)^2, \quad (2.13)$$

$$\int d^3\mathbf{x} e^{i\mathbf{q}\cdot\mathbf{x}} \langle \theta_{33}(x) \theta_{33}(0) \rangle_0 = \frac{2d_A e^{-qx_0}}{15(4\pi)^2 x_0^5} (24 + 24qx_0 + 12q^2 x_0^2 + 4q^3 x_0^3 + q^4 x_0^4), \quad (2.14)$$

$$\rho_{33,33}(\omega, q) = \frac{2d_A \theta(\omega - q)}{15(4\pi)^2} \omega^4, \quad (2.15)$$

$$\int d^3\mathbf{x} e^{i\mathbf{q}\cdot\mathbf{x}} \langle \theta(x) \theta(0) \rangle_0 = \left(\frac{11\alpha_s N_c}{6\pi} \right)^2 \frac{2d_A e^{-qx_0}}{(4\pi)^2 x_0^5} (3 + 3qx_0 + q^2 x_0^2), \quad (2.16)$$

$$\rho_{\theta,\theta}(\omega, q) = \left(\frac{11\alpha_s N_c}{6\pi} \right)^2 \frac{d_A \theta(\omega - q)}{4(4\pi)^2} (\omega^2 - q^2)^2. \quad (2.17)$$

$$\int d^3\mathbf{x} e^{i\mathbf{q}\cdot\mathbf{x}} \langle \theta_{00}(x) \theta_{00}(0) \rangle_0 = \frac{2d_A q^4 e^{-qx_0}}{15(4\pi)^2 x_0} \quad (2.18)$$

$$\rho_{00,00}(\omega, q) = \frac{2d_A \theta(\omega - q)}{15(4\pi)^2} q^4. \quad (2.19)$$

2.2 Finite temperature

The $\mathbf{q} = 0$ correlation functions of interest are

$$\int d^3\mathbf{x} \langle \theta_{00}(0) \theta_{00}(x) \rangle_0 = \frac{4\pi^2 d_A T^5}{15}, \quad (2.20)$$

$$\int d^3\mathbf{x} \langle \theta(0) \theta_{00}(x) \rangle_0 = 0, \quad (2.21)$$

$$\int d^3\mathbf{x} \langle \theta(0) \theta(x) \rangle_0 = \left(\frac{11\alpha_s N_c}{6\pi} \right)^2 \frac{16d_A T^5}{\pi^2} \left(f(\tau) - \frac{\pi^4}{60} \right), \quad (2.22)$$

$$\int d^3\mathbf{x} \langle \theta_{12}(0) \theta_{12} \rangle_0 = \frac{32d_A T^5}{5\pi^2} \left(f(\tau) - \frac{\pi^4}{72} \right), \quad (2.23)$$

$$\int d^3\mathbf{x} \langle \theta_{11}(0) \theta_{11} \rangle_0 = \frac{128d_A T^5}{15\pi^2} \left(f(\tau) - \frac{\pi^4}{96} \right), \quad (2.24)$$

where $\tau = 1 - 2Tx_0$ and

$$f(\tau) = \int_0^\infty ds s^4 \frac{\cosh^2 \tau s}{\sinh^2 s} = \frac{\pi^4}{60} + \frac{3}{4} \sum_{n \geq 1} \frac{n}{(n-\tau)^5} + \frac{n}{(n+\tau)^5}. \quad (2.25)$$

The two point function of $\int d^3\mathbf{x} T_{00}(x)$ is time-independent, as expected for a conserved charge. The spectral functions in the tensor and scalar channels read (see for instance [34, 26])

$$\rho_{12,12}(\omega, \mathbf{0}, T) = \frac{d_A}{10(4\pi)^2} \frac{\omega^4}{\tanh \frac{\omega}{4T}} + \left(\frac{2\pi}{15} \right)^2 d_A T^4 \omega \delta(\omega) \quad (2.26)$$

$$\rho_{\theta,\theta}(\omega, \mathbf{0}, T) = \frac{d_A}{4(4\pi)^2} \left(\frac{11\alpha_s N_c}{6\pi} \right)^2 \frac{\omega^4}{\tanh \frac{\omega}{4T}}. \quad (2.27)$$

2.2.1 Finite momentum

For a polynomial P , we define

$$\mathcal{I}([P], \omega, q, T) = \theta(\omega - q) \int_0^1 dz \frac{P(z) \sinh \frac{\omega}{2T}}{\cosh \frac{\omega}{2T} - \cosh \frac{qz}{2T}} + \theta(q - \omega) \int_1^\infty dz \frac{P(z) \sinh \frac{\omega}{2T}}{\cosh \frac{qz}{2T} - \cosh \frac{\omega}{2T}}. \quad (2.28)$$

Then the spectral functions read

$$\rho_{13,13}(\omega, q, T) = \frac{d_A}{8(4\pi)^2} \omega^2 (\omega^2 - q^2) \mathcal{I}([1 - z^4], \omega, q, T), \quad (2.29)$$

$$\rho_{12,12}(\omega, q, T) = \frac{d_A}{32(4\pi)^2} (\omega^2 - q^2)^2 \mathcal{I}([1 + 6z^2 + z^4], \omega, q, T), \quad (2.30)$$

$$\rho_{33,33}(\omega, q, T) = \frac{d_A}{4(4\pi)^2} \omega^4 \mathcal{I}([(1 - z^2)^2], \omega, q, T), \quad (2.31)$$

$$\rho_{\theta,\theta}(\omega, q, T) = \left(\frac{11\alpha_s N_c}{6\pi} \right)^2 \frac{d_A}{4(4\pi)^2} (\omega^2 - q^2)^2 \mathcal{I}([1], \omega, q, T), \quad (2.32)$$

$$\rho_{00,00}(\omega, q, T) = \frac{d_A}{4(4\pi)^2} q^4 \mathcal{I}([(1 - z^2)^2], \omega, q, T), \quad (2.33)$$

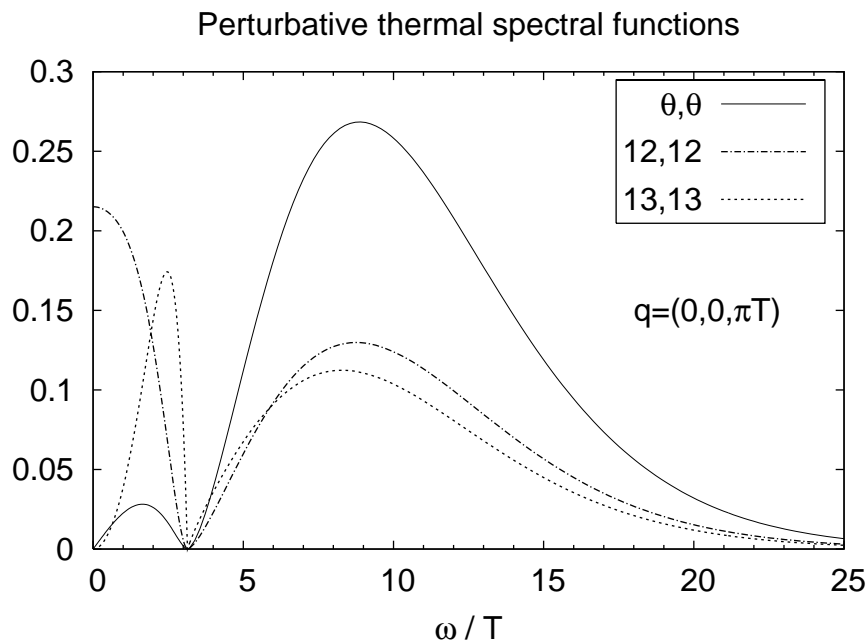


Figure 1: The function $\frac{1}{d_A T^4} [\rho(\omega, \mathbf{q}, T) / \tanh(\omega/2T) - \rho(\omega, \mathbf{q}, 0)]$ for $q = \pi T$. For the trace anomaly θ , the factor $(11\alpha_s N_c / 6\pi)^2$ has been dropped.

$$-\rho_{01,01}(\omega, q, T) = \frac{d_A}{8(4\pi)^2} q^2(\omega^2 - q^2) \mathcal{I}([(1 - z^4)], \omega, q, T), \quad (2.34)$$

$$-\rho_{03,03}(\omega, q, T) = \frac{d_A}{4(4\pi)^2} q^2 \omega^2 \mathcal{I}([(1 - z^2)^2], \omega, q, T). \quad (2.35)$$

One finds that

$$\mathcal{I}([1], \omega, q, T) = -\frac{\omega}{q} \theta(q - \omega) + \frac{2T}{q} \log \frac{\sinh(\omega + q)/4T}{\sinh|\omega - q|/4T} \quad (2.36)$$

and hence the trace anomaly correlator can be expressed in terms of elementary functions. The integrals with z^2 and z^4 in the numerator can be expressed in terms of polylogarithms, explicit formulas are given in appendix C. A few spectral functions are displayed on figure 1.

3. Physics discussion

At small momentum and frequency, the expression for the spectral functions of the momentum densities are predicted by hydrodynamics (see [35] for an explicit derivation),

$$\frac{\rho_{01,01}(\omega, \mathbf{q})}{\omega} \underset{\omega, q \rightarrow 0}{\sim} \frac{\eta}{\pi} \frac{q^2}{\omega^2 + (\eta q^2 / (Ts))^2}, \quad (3.1)$$

$$\frac{\rho_{03,03}(\omega, \mathbf{q})}{\omega} \underset{\omega, q \rightarrow 0}{\sim} \frac{\frac{4}{3}\eta + \zeta}{\pi} \frac{\omega^2 q^2}{(\omega^2 - v_s^2 q^2)^2 + (\omega q^2 (\frac{4}{3}\eta + \zeta) / (Ts))^2}, \quad (3.2)$$

where s is the entropy density, v_s is the velocity of sound and $\mathbf{q} = q\hat{e}_3$.

Based on the fact the matrix elements of $\partial_\mu T^{\mu\nu}$ vanish between any two on-shell states, the Euclidean correlators of the charges and those of the fluxes are related in a simple way. We emphasize that these relations are exact, since they derive from a Ward identity. In terms of the spectral functions they read ($\mathbf{q} = q\hat{e}_3$)

$$\omega^4 \rho_{00,00}(\omega, \mathbf{q}) = q^4 \rho_{33,33}(\omega, \mathbf{q}) \tag{3.3}$$

$$-\omega^2 \rho_{01,01}(\omega, \mathbf{q}) = q^2 \rho_{13,13}(\omega, \mathbf{q}) \tag{3.4}$$

$$-\omega^2 \rho_{03,03}(\omega, \mathbf{q}) = q^2 \rho_{33,33}(\omega, \mathbf{q}). \tag{3.5}$$

These relations are in particular satisfied by our treelevel expressions, eq. (2.29)–(2.35). Note that the minus signs on the right-hand side of eq. (3.4)–(3.5) are absent in Minkovsky space (they come from the definition of T_{0k} itself, see the remark at the beginning of section 2).

Equations (3.4)–(3.5) and (3.1)–(3.2) can be combined to obtain (1.2) and (1.3), which have so far been the basis of the calculation of shear and bulk viscosity using lattice Monte-Carlo techniques [26–28, 17]. In that strategy, the momentum \mathbf{q} is set to zero at the outset, and ω is sent to zero at the end.

However, in view of eq. (3.1)–(3.2), the shear and bulk viscosity can be extracted from the low-frequency behavior of the spectral functions for the four charge densities $T_{0\mu}$, as long as $\mathbf{q} \neq 0$. The advantage of using these correlators is that the ultraviolet contributions are highly suppressed compared to the correlators of the spatial components. We may illustrate this point by two numerical examples.

In eq. (2.26), relevant to shear viscosity, the $\omega^4 / \tanh \frac{\omega}{4T}$ term contributes for 86% to the Euclidean correlator at $t = 1/2T$. By contrast, in the $\rho_{01,01}$ channel for $q = \pi T/2$, the contributions to $C_E(x_0 = 1/2T)/(d_A T^5)$ coming from $\omega > q$ and $\omega < q$ are respectively ≈ 0.04 and 0.6 , assuming the treelevel form (eq. 2.34) in the first region and eq. (3.1) with $s = \frac{3}{4}s_{\text{SB}} = \frac{1}{15}d_A \pi^2 T^3$ and $\eta/s = 1/4\pi$ in the second.

In the energy density channel, the increase in sensitivity to the low-frequency region of the spectral function is even more dramatic: for $q = \pi T/2$, the contribution to $C_E(x_0 = 1/2T)/(d_A T^5)$ from $\omega > q$ is merely ≈ 0.01 based on eq. (2.33), while the sub-threshold contribution is about 1.9 for $s = \frac{3}{4}s_{\text{SB}}$, $v_s^2 = \frac{1}{3}$, $\eta/s = 1/4\pi$ and $\zeta = 0$. These values are inspired by the strongly coupled $\mathcal{N} = 4$ SU(N_c) SYM gauge theory, which can be studied by analytic AdS/CFT methods (see for instance [36] and ref. therein).

One of the key issues in practice is to achieve sufficiently small q for the hydrodynamics prediction to be valid below threshold. One will want to reach $q < \pi T/2$ and check this explicitly. Since $q = 2\pi/L$ is the smallest momentum available in a periodic box, this requires simulating in rather large spatial volumes. Approaching a second order phase transition, it may become impractical to reach sufficiently small momenta. Anisotropic lattices [37, 18] can help to achieve large physical volumes while keeping discretization errors under control. From the algorithmic point of view, having a non-zero spatial momentum is a particularly favorable situation for the multi-level algorithm [38–40], since it allows the ultraviolet fluctuations to be tamed very efficiently. Indeed non-perturbative, non-zero momentum correlators of the momentum fluxes were presented with 1% precision in [18].

In the case of the vector current $\bar{\psi}\gamma_\mu\psi$, it may also be profitable to exploit the correlator of the charge density with non-zero momentum. Non-zero momentum correlators of the current have been computed with good precision [41], exploiting twisted boundary conditions to scan low momenta more easily.

Acknowledgments

This work was supported in part by funds provided by the U.S. Department of Energy under cooperative research agreement DE-FG02-94ER40818.

A. Calculation of Euclidean correlators

In this appendix we derive a form of the Euclidean correlators which is well suited for accurate numerical evaluation. We start with $\langle T_{12}(0) T_{12}(x) \rangle$, and then give results for other channels treated in the same way. The orientation of the momentum is specified by $\mathbf{q} = q\hat{e}_i$, $i = 1, 2, 3$. The color factor d_A is omitted.

A.1 The $\langle T_{12}(0) T_{12}(x) \rangle$ correlator

$$\begin{aligned} \langle T_{12}(0) T_{12}(x) \rangle &= \langle (F_{10}F_{20})(0) (F_{10}F_{20})(x) \rangle + \langle (F_{13}F_{23})(0) (F_{13}F_{23})(x) \rangle \\ &\quad + 2 \langle (F_{10}F_{20})(0) (F_{13}F_{23})(x) \rangle. \end{aligned} \quad (\text{A.1})$$

Explicitly, the tensor $\tilde{\phi}_{\mu\nu\alpha\beta}$ reads

$$\tilde{\phi}_{\mu\nu\alpha\beta}(\mathbf{p}, x_0) = \frac{1}{L_0} \sum_{p_0} \frac{e^{ip_0x_0}}{p_0^2 + \mathbf{p}^2} \left[\delta_{\nu\beta} p_\mu p_\alpha + \delta_{\mu\alpha} p_\nu p_\beta - \delta_{\mu\beta} p_\nu p_\alpha - \delta_{\nu\alpha} p_\mu p_\beta \right].$$

In the $T \rightarrow 0$ limit of course one can make the substitution $\frac{1}{L_0} \sum_{p_0} \rightarrow \int \frac{dp_0}{2\pi}$. Defining

$$\mathcal{A} = \frac{1}{L_0^2} \sum_{p_0, q_0} \int \frac{d^3\mathbf{p}}{(2\pi)^3} (p_1^2 + p_0^2) \frac{e^{ip_0x_0}}{p_0^2 + \mathbf{p}^2} ((p_2 + q_2)^2 + q_0^2) \frac{e^{iq_0x_0}}{q_0^2 + (\mathbf{p} + \mathbf{q})^2}, \quad (\text{A.2})$$

$$\mathcal{B} = \frac{1}{L_0^2} \sum_{p_0, q_0} \int \frac{d^3\mathbf{p}}{(2\pi)^3} p_1 p_2 \frac{e^{ip_0x_0}}{p_0^2 + \mathbf{p}^2} (p_1 + q_1)(p_2 + q_2) \frac{e^{iq_0x_0}}{q_0^2 + (\mathbf{p} + \mathbf{q})^2}, \quad (\text{A.3})$$

$$\mathcal{C} = \frac{1}{L_0^2} \sum_{p_0, q_0} \int \frac{d^3\mathbf{p}}{(2\pi)^3} (p_1^2 + p_3^2) \frac{e^{ip_0x_0}}{p_0^2 + \mathbf{p}^2} [(p_2 + q_2)^2 + (p_3 + q_3)^2] \frac{e^{iq_0x_0}}{q_0^2 + (\mathbf{p} + \mathbf{q})^2}, \quad (\text{A.4})$$

$$\mathcal{D} = \frac{-1}{L_0^2} \sum_{p_0, q_0} \int \frac{d^3\mathbf{p}}{(2\pi)^3} p_0 p_3 \frac{e^{ip_0x_0}}{p_0^2 + \mathbf{p}^2} q_0 (p_3 + q_3) \frac{e^{iq_0x_0}}{q_0^2 + (\mathbf{p} + \mathbf{q})^2}, \quad (\text{A.5})$$

we have

$$\int d^3\mathbf{x} e^{i\mathbf{q}\cdot\mathbf{x}} \langle F_{10}F_{20} \rangle(0) \langle F_{10}F_{20} \rangle(x) = \mathcal{A} + \mathcal{B}, \quad (\text{A.6})$$

$$\int d^3\mathbf{x} e^{i\mathbf{q}\cdot\mathbf{x}} \langle F_{13}F_{23} \rangle(0) \langle F_{13}F_{23} \rangle(x) = \mathcal{B} + \mathcal{C}, \quad (\text{A.7})$$

$$\int d^3\mathbf{x} e^{i\mathbf{q}\cdot\mathbf{x}} \langle F_{10}F_{20} \rangle(0) \langle F_{13}F_{23} \rangle(x) = \mathcal{D}. \quad (\text{A.8})$$

Using the Poisson summation formula, we obtain

$$\mathcal{A} = \frac{1}{4} \sum_{m,n \in \mathbf{Z}} \int \frac{d^3 \mathbf{p}}{(2\pi)^3} \frac{(p_1^2 - \mathbf{p}^2) ((p_2 + q_2)^2 - (\mathbf{p} + \mathbf{q})^2)}{|\mathbf{p}| |\mathbf{p} + \mathbf{q}|} e^{-|\mathbf{p}| |x_0 + mL_0|} e^{-|\mathbf{p} + \mathbf{q}| |x_0 + nL_0|}, \quad (\text{A.9})$$

$$\mathcal{B} = \frac{1}{4} \sum_{m,n \in \mathbf{Z}} \int \frac{d^3 \mathbf{p}}{(2\pi)^3} \frac{p_1 p_2 (p_1 + q_1)(p_2 + q_2)}{|\mathbf{p}| |\mathbf{p} + \mathbf{q}|} e^{-|\mathbf{p}| |x_0 + mL_0|} e^{-|\mathbf{p} + \mathbf{q}| |x_0 + nL_0|}, \quad (\text{A.10})$$

$$\mathcal{C} = \frac{1}{4} \sum_{m,n \in \mathbf{Z}} \int \frac{d^3 \mathbf{p}}{(2\pi)^3} \frac{(p_1^2 + p_3^2) [(p_2 + q_2)^2 + (p_3 + q_3)^2]}{|\mathbf{p}| |\mathbf{p} + \mathbf{q}|} e^{-|\mathbf{p}| |x_0 + mL_0|} e^{-|\mathbf{p} + \mathbf{q}| |x_0 + nL_0|}, \quad (\text{A.11})$$

$$\mathcal{D} = \frac{1}{4} \sum_{m,n \in \mathbf{Z}} s_m \left(\frac{x_0}{L_0} \right) s_n \left(\frac{x_0}{L_0} \right) \int \frac{d^3 \mathbf{p}}{(2\pi)^3} p_3 (p_3 + q_3) e^{-|\mathbf{p}| |x_0 + mL_0|} e^{-|\mathbf{p} + \mathbf{q}| |x_0 + nL_0|}, \quad (\text{A.12})$$

where

$$s_n(x) \equiv \text{sign}(x + n). \quad (\text{A.13})$$

Integrating in spherical coordinates leads to

$$\begin{aligned} \int d^3 x e^{i\mathbf{q} \cdot \mathbf{x}} \langle T_{12}(0) T_{12}(x) \rangle &= \frac{q^5}{64\pi^2} \sum_{m,n \in \mathbf{Z}} \int_0^\infty k^3 dk e^{-|x_0 + mL_0|k} \times \\ &\times \left\{ k \sqrt{k^2 + 1} (J_{\mathcal{A}} + 2J_{\mathcal{B}} + J_{\mathcal{C}}) \left(q|x_0 + nL_0| \sqrt{k^2 + 1}, \frac{2k}{k^2 + 1}, k \right) \right. \\ &\left. + 2(k^2 + 1) s_m \left(\frac{x_0}{L_0} \right) s_n \left(\frac{x_0}{L_0} \right) I_{\mathcal{D}} \left(q|x_0 + nL_0| \sqrt{k^2 + 1}, \frac{2k}{k^2 + 1}, k \right) \right\}, \end{aligned} \quad (\text{A.14})$$

where

$$J_{\mathcal{A},\mathcal{B},\mathcal{C}}(x, A, k) = \int_{-A}^A \frac{dy}{\sqrt{1+y}} e^{-x\sqrt{1+y}} P_{\mathcal{A},\mathcal{B},\mathcal{C}}(y/A, k) \quad (\text{A.15})$$

$$I_{\mathcal{D}}(x, A, k) = \int_{-A}^A dy e^{-x\sqrt{1+y}} P_{\mathcal{D}}(y/A, k). \quad (\text{A.16})$$

Via the change of variables $u = \sqrt{1+y}$, these integrals can be obtained in terms of the function

$$g(x, A) \equiv \frac{1}{x} \left(e^{-x\sqrt{1-A}} - e^{-x\sqrt{1+A}} \right). \quad (\text{A.17})$$

We have

$$J_{\mathcal{A},\mathcal{B},\mathcal{C}}(x, A, k) = 2P_{\mathcal{A},\mathcal{B},\mathcal{C}} \left(A^{-1} \left(\frac{d^2}{dx^2} - 1 \right), k \right) g(x, A) \quad (\text{A.18})$$

$$I_{\mathcal{D}}(x, A, k) = -2 \frac{d}{dx} P_{\mathcal{D}} \left(A^{-1} \left(\frac{d^2}{dx^2} - 1 \right), k \right) g(x, A) \quad (\text{A.19})$$

Note that $\sqrt{1 \pm A} = \frac{|k \pm 1|}{\sqrt{k^2 + 1}}$ for $A = \frac{2k}{k^2 + 1}$.

One then obtains the correlator in the form

$$\int d^3 x e^{i\mathbf{q} \cdot \mathbf{x}} \langle T_{12}(0) T_{12}(x) \rangle = \frac{q^5}{\pi^2} \sum_{n,m \in \mathbf{Z}} g \left([\text{II}]; s_m \left(\frac{x_0}{L_0} \right) s_n \left(\frac{x_0}{L_0} \right), q|x_0 + mL_0|, q|x_0 + nL_0| \right), \quad (\text{A.20})$$

where

$$g([\Pi]; s, x, y) = \frac{e^{-x} \Pi(s, x, y) - e^{-y} \Pi(s, y, x)}{(x^2 - y^2)^5} = g([\Pi]; s, y, x) \quad (\text{A.21})$$

and the appropriate polynomials Π will be specified below for a few cases of interest. The function g will always be finite at $x = y$, and we give the first two terms in the expansion around this point, which is useful when implementing expression (A.20) numerically. Since the series in n and m are exponentially convergent, only a few terms are needed to reach, say, a precision of 10^{-6} .

Consider the case $\mathbf{q} = (q, 0, 0)$, $q \geq 0$. Relabelling the p -coordinates $p_1 \rightarrow p_3$, $p_3 \rightarrow p_2$, $p_2 \rightarrow p_1$ in eq. (A.12) before going to spherical coordinates, we obtain,

$$P_{\mathcal{A}}(y, k) = (1 - y^2) \left(y^2 + \frac{4}{k}y + \frac{2}{k^2} + 1 \right), \quad (\text{A.22})$$

$$P_{\mathcal{B}}(y, k) = y(1 - y^2) \left(y + \frac{1}{k} \right), \quad (\text{A.23})$$

$$P_{\mathcal{C}}(y, k) = 1 - y^4, \quad (\text{A.24})$$

$$P_{\mathcal{D}}(y, k) = 1 - y^2, \quad (\text{A.25})$$

and from there

$$\begin{aligned} 2 \Pi_{12,12}^{\hat{\epsilon}_1}(s, x, y) &= 4608 + x(6 + x)(768 + x(240 + x(72 + x(10 + x)))) \quad (\text{A.26}) \\ &\quad - 4sx(48 + x(48 + x(12 + x)))y \\ &\quad - (96 + x(96 + x(120 + x(32 + 3x))))y^2 \\ &\quad + 8sx(6 + x)y^3 + (6 + x)(-2 + 3x)y^4 - 4sy^5 - y^6, \\ g([\Pi_{12,12}^{\hat{\epsilon}_1}]; s, x + \frac{1}{2}\epsilon, x - \frac{1}{2}\epsilon) &= \frac{e^{-x}}{240x^5} \left\{ x^3(2 + s) + 3(7 + 5s) + 3x(7 + 5s) + x^2(9 + 6s) \right. \\ &\quad \left. + \frac{\epsilon^2}{56} \left((39 + 21s + x^3(4 + s) + 3x(13 + 7s) + x^2(17 + 8s)) \right) \right. \\ &\quad \left. + O(\epsilon^4) \right\}. \quad (\text{A.27}) \end{aligned}$$

In eq. (A.27), we have defined g by continuity.

For the case $\mathbf{q} = (0, 0, q)$, $q \geq 0$, we obtain

$$P_{\mathcal{A}}(y, k) = \frac{1}{4}y^4 + \frac{2}{k}y^3 + \left(\frac{1}{k^2} + \frac{3}{2} \right) y^2 + \frac{2}{k}y + \frac{1}{k^2} + \frac{1}{4}, \quad (\text{A.28})$$

$$P_{\mathcal{B}}(y, k) = \frac{1}{4}(1 - y^2)^2, \quad (\text{A.29})$$

$$P_{\mathcal{C}}(y, k) = P_{\mathcal{A}}(y), \quad (\text{A.30})$$

$$P_{\mathcal{D}}(y, k) = 2y \left(y + \frac{1}{k} \right), \quad (\text{A.31})$$

and further

$$\Pi_{12,12}^{\hat{e}_3}(s, x, y) = -576 - x(4+x)(144+x(48+x(24+x(6+x)))) \quad (\text{A.32})$$

$$\begin{aligned} & + 2sx(96+x(96+x(48+x(11+x))))y \\ & + (-48+x(-48+x(-48+(-4+x)x)))y^2 \\ & - 4sx^2(5+x)y^3 + x(14+x)y^4 + 2s(-1+x)y^5 - y^6. \end{aligned}$$

$$\begin{aligned} g\left(\left[\Pi_{12,12}^{\hat{e}_3}\right]; s, x + \frac{1}{2}\epsilon, x - \frac{1}{2}\epsilon\right) &= \frac{e^{-x}}{240x^5} \left\{ 21 + x(21+x(9+x(2+x))) \right. \\ & + s(15-x(-15+(-1+x)x(3+x))) \\ & + \frac{\epsilon^2}{56} \left(69 - 2x^3(-1+s) - x^4(-1+s) + 63s \right. \\ & \left. \left. + x^2(25+19s) + x(69+63s) \right) + O(\epsilon^4) \right\}. \end{aligned} \quad (\text{A.33})$$

Note that the polynomials $P_{A,B,C,D}(y, k)$ all have the symmetry $P_{A,B,C,D}(-y, -k) = P_{A,B,C,D}(y, k)$.

A.2 $\langle T_{11}T_{11} \rangle$ with momentum along x direction

For $\int d^3\mathbf{x} e^{i\mathbf{q}\cdot\mathbf{x}} \langle T_{11}(0)T_{11}(x) \rangle$, the polynomial is

$$\begin{aligned} -\Pi_{11,11}^{\hat{e}_1}(s, x, y) &= 4608 + x(4608 + x(2112 + x(576 + x(108 + x(14 + x)))) \\ & + sx(2+x)(120+x(60+x(12+x)))y \\ & - (192+x(192+x(24+x(4+x))))y^2 - 2sx(18+x(8+x))y^3 \\ & - (-12+x(10+x))y^4 + s(2+x)y^5 + y^6, \end{aligned} \quad (\text{A.34})$$

$$\begin{aligned} g\left(\left[\Pi_{11,11}^{\hat{e}_1}\right]; s, x + \frac{1}{2}\epsilon, x - \frac{1}{2}\epsilon\right) &= \frac{e^{-x}}{480x^5} \left\{ 66(1+x) + 2x^2(15+x(4+x)) + \right. \\ & + s(30+x(30+x(15+x(5+x)))) \\ & + \frac{\epsilon^2}{56} \left(138 + 138x + x^4(2+s) + x^3(8+5s) + x^2(54+5s) \right) \\ & \left. + O(\epsilon^4) \right\}. \end{aligned} \quad (\text{A.35})$$

A.3 Scalar correlator with non-zero momentum

For $\frac{1}{4} \sum_{\mu < \nu, \rho < \sigma} \int d^3\mathbf{x} e^{i\mathbf{q}\cdot\mathbf{x}} \langle F_{\mu\nu}^2(0)F_{\rho\sigma}^2(x) \rangle$, the polynomial is

$$\begin{aligned} -\Pi_{\theta,\theta}^{\hat{e}_3}(s, x, y) &= x^4(12+x(6+x)) - 2sx^3(24+x(9+x))y \\ & - x^2(-72+(-12+x)x)y^2 + 4sx(-12+x(3+x))y^3 \\ & - (-12+x(18+x))y^4 - 2s(-3+x)y^5 + y^6. \end{aligned} \quad (\text{A.36})$$

$$\begin{aligned} g\left(\left[\Pi_{\theta,\theta}^{\hat{e}_3}\right]; s, x + \frac{1}{2}\epsilon, x - \frac{1}{2}\epsilon\right) &= \frac{e^{-x}}{240x^5} \left\{ -x^4(-1+s) + 45(1+s) + 45x(1+s) + 15x^2(1+s) \right. \\ & \left. + \frac{\epsilon^2}{56} \left(-x^4(-1+s) + 105(1+s) + 105x(1+s) + 35x^2(1+s) \right) + O(\epsilon^4) \right\}. \end{aligned} \quad (\text{A.37})$$

B. Calculation of spectral functions

In this appendix, we show how to obtain eq. (2.29)–(2.35) in the case of the $\langle T_{12}T_{12} \rangle$ correlator. Other cases can be treated in exactly the same way. In this section q is understood to be in units of $2T$. Using the propagator in the mixed representation,

$$\frac{1}{L_0} \sum_{p_0} \frac{e^{ip_0 x_0}}{p_0^2 + \mathbf{p}^2} = \frac{1}{2|\mathbf{p}|} \frac{\cosh |\mathbf{p}|(\frac{1}{2}L_0 - x_0)}{\sinh \frac{1}{2}|\mathbf{p}|L_0}, \quad (\text{B.1})$$

we obtain ($\tau = 1 - 2Tx_0$)

$$\begin{aligned} \mathcal{A}, \mathcal{B}, \mathcal{C} = & \frac{1}{\pi^2 L_0^5} \int_0^\infty p^4 dp \int_{-1}^1 dx \frac{p}{p^2 + q^2 + 2pqx} P_{\mathcal{A}, \mathcal{B}, \mathcal{C}} \left(x, \frac{p}{q} \right) \\ & \frac{\cosh(p + \sqrt{p^2 + q^2 + 2pqx})\tau + \cosh(p - \sqrt{p^2 + q^2 + 2pqx})\tau}{\cosh(p + \sqrt{p^2 + q^2 + 2pqx}) - \cosh(p - \sqrt{p^2 + q^2 + 2pqx})}. \end{aligned} \quad (\text{B.2})$$

For the term proportional to $\cosh(p + \sqrt{p^2 + q^2 + 2pqx})\tau$, we do the change of variables $p = \frac{p^2 - q^2}{2(k+qx)}$, which brings this expression to the desired form $\cosh(k\tau)$ on the integration interval $k|_q^\infty$.

For the $\cosh(p - \sqrt{p^2 + q^2 + 2pqx})\tau$ term, we choose $p = \frac{k^2 - q^2}{2(qx - k)}$, which achieves the same on the integration interval $k|_{qx}^q$. We then notice that if $\mathcal{F}(-x, -k, q) = \mathcal{F}(x, k, q)$,

$$\int_{-1}^1 dx \int_{qx}^q dk \mathcal{F}(x, k, q) = \int_0^q \int_{-1}^1 \mathcal{F}(x, -k, q).$$

One therefore finds that the first term determines the spectral function above the threshold q , while the second determines it below q . We write

$$\rho(\omega, q, T) = \rho_{<}(\omega, q, T) + \rho_{>}(\omega, q, T), \quad (\text{B.3})$$

where the first term vanishes for $\omega > q$ and the second for $\omega < q$.

After some algebra,

$$\begin{aligned} \rho_{\mathcal{A}, \mathcal{B}, \mathcal{C}, >}(2kT, 2qT, T) = & \frac{T^4 \theta(k - q) \sinh k (k^2 - q^2)^5}{64\pi^2} \\ & \int_{-1}^1 dx \frac{P_{\mathcal{A}, \mathcal{B}, \mathcal{C}}(x, \frac{k^2 - q^2}{2q(k+qx)})}{(k + qx)^6} \frac{1}{\cosh k - \cosh q \frac{q+kx}{k+qx}}. \end{aligned} \quad (\text{B.4})$$

and after the further change of variables $x = \frac{kz - q}{k - qz}$, we obtain

$$\begin{aligned} \rho_{\mathcal{A}, \mathcal{B}, \mathcal{C}, >}(2kT, 2qT, T) = & \frac{T^4 \theta(k - q) \sinh k}{64\pi^2} \\ & \int_{-1}^1 \frac{dz (k - qz)^4}{\cosh k - \cosh qz} P_{\mathcal{A}, \mathcal{B}, \mathcal{C}} \left(\frac{kz - q}{k - qz}, \frac{k - qz}{2q} \right). \end{aligned} \quad (\text{B.5})$$

After the change of variables $p = p(k)$ but before the change of variables $x = x(z)$, the sub-threshold part, $\rho_{<}(2kT, 2qT, T)$, has the same expression as $\rho_{>}$. However, in

order to perform the change of variables $x(z)$, the integral must first be split, $\int_{-1}^1 dx = \int_{-1}^{-k/q} dx + \int_{-k/q}^1 dx$. These integration intervals are mapped to the z -integrals $\int_{-\infty}^{-1}$ and \int_1^{∞} . Because $\frac{dx}{dz} < 0$ on these two intervals, a minus sign relative to $\rho_>$ appears. One thus finds

$$\rho_{\mathcal{A},\mathcal{B},\mathcal{C},<}(2kT, 2qT, T) = \frac{T^4 \theta(q-k) \sinh k}{64\pi^2} \left(\int_{-\infty}^{-1} + \int_1^{\infty} \right) \frac{dz(k-qz)^4}{\cosh qz - \cosh k} P_{\mathcal{A},\mathcal{B},\mathcal{C}} \left(\frac{kz-q}{k-qz}, \frac{k-qz}{2q} \right). \quad (\text{B.6})$$

For the contribution

$$\mathcal{D} = \frac{T^5}{\pi^2} \int_{-1}^1 \int_0^{\infty} dp p^4 P_{\mathcal{D}} \left(x, \frac{p}{q} \right) \frac{\cosh(p + \sqrt{p^2 + q^2 + 2pqx})\tau - \cosh(p - \sqrt{p^2 + q^2 + 2pqx})\tau}{\cosh(p + \sqrt{p^2 + q^2 + 2pqx}) - \cosh(p - \sqrt{p^2 + q^2 + 2pqx})} \quad (\text{B.7})$$

we follow exactly the same steps as for $\mathcal{A}, \mathcal{B}, \mathcal{C}$ and find

$$\rho_{\mathcal{D},>}(2kT, 2qT, T) = \frac{T^4 \theta(k-q) \sinh k}{64\pi^2} \int_{-1}^1 \frac{dz(k-qz)^2(k^2 - q^2 z^2)}{\cosh k - \cosh qz} P_{\mathcal{D}} \left(\frac{kz-q}{k-qz}, \frac{k-qz}{2q} \right). \quad (\text{B.8})$$

For the sub-threshold part (which includes the minus sign in the numerator of eq. (B.7)) we find the same expression as for $\rho_>$ before the change of variables $x(z)$. Therefore, again, in the final expression $\rho_<$ has a relative minus sign as well as the complementary integration range as compared to $\rho_>$,

$$\rho_{\mathcal{D},<}(2kT, 2qT, T) = \frac{T^4 \theta(q-k) \sinh k}{64\pi^2} \left(\int_{-\infty}^{-1} + \int_1^{\infty} \right) \frac{dz(k-qz)^2(k^2 - q^2 z^2)}{\cosh qz - \cosh k} P_{\mathcal{D}} \left(\frac{kz-q}{k-qz}, \frac{k-qz}{2q} \right). \quad (\text{B.9})$$

Finally, in view of the symmetry $P(-y, -k) = P(y, k)$ of the relevant polynomials, \int_{-1}^1 can be replaced by $2 \int_0^1$ and $\int_{-\infty}^{-1} + \int_1^{\infty}$ by $2 \int_1^{\infty}$.

C. The spectral function in terms of polylogarithms

Polylogarithms are defined by the series $\text{Li}_n(z) = \sum_{k \geq 1} \frac{z^k}{k^n}$ and analytic continuation thereof. The integrals appearing in the spectral function are given as follows in terms of these special functions:

$$\begin{aligned} q^3 \mathcal{I}([z^2]; 2T_w, 2T_q, T) &= -q^2 \left((\log(1 - e^{q-w}) - \log(e^{w+q} - 1)) \right. \\ &\quad - 2q \left(\text{Li}_2(e^{q-w}) - \text{Li}_2(e^{w+q}) \right) + 2 \left(\text{Li}_3(e^{q-w}) - \text{Li}_3(e^{w+q}) \right) \\ &\quad \left. + i\pi q^2 - \frac{1}{3} (1 + \theta(q-w)) (w^3 - 2\pi^2 w + 3i\pi w^2) \right) \end{aligned} \quad (\text{C.1})$$

$$q^5 \mathcal{I}([z^4]; 2T_w, 2T_q, T) = -q^4 \left(\log(1 - e^{q-w}) - \log(e^{q+w} - 1) \right) \quad (\text{C.2})$$

$$\begin{aligned}
 & -4q^3 (\text{Li}_2(e^{q-w}) - \text{Li}_2(e^{w+q})) + 12q^2 (\text{Li}_3(e^{q-w}) - \text{Li}_3(e^{q+w})) \\
 & -24q (\text{Li}_4(e^{q-w}) - \text{Li}_4(e^{q+w})) + 24 (\text{Li}_5(e^{q-w}) - \text{Li}_5(e^{q+w})) \\
 & + i\pi q^4 - \frac{1}{15} (1 + \theta(q-w)) (3w^5 - 20\pi^2 w^3 - 8\pi^4 w + 15i\pi w^4)
 \end{aligned}$$

The integral with z^0 in the numerator can be expressed in terms of elementary functions, see eq. (2.36). Hence in all cases the expressions on the left and on the right of the threshold differ by a polynomial in ω . In order to simplify expressions eq. (C.1) and (C.2), we have used the identities

$$\text{Li}_5(e^{-w}) - \text{Li}_5(e^w) = \frac{w^5}{120} - \frac{\pi^2}{18} w^3 - \frac{\pi^4}{45} w + \frac{i\pi}{24} w^4 \quad (\text{C.3})$$

$$\text{Li}_3(e^{-w}) - \text{Li}_3(e^w) = \frac{w^3}{6} - \frac{\pi^2}{3} w + \frac{i\pi}{2} w^2. \quad (\text{C.4})$$

References

- [1] BRAHMS collaboration, I. Arsene et al., *Quark gluon plasma and color glass condensate at RHIC? The perspective from the BRAHMS experiment*, *Nucl. Phys. A* **757** (2005) 1 [nucl-ex/0410020].
- [2] B.B. Back et al., *The PHOBOS perspective on discoveries at RHIC*, *Nucl. Phys. A* **757** (2005) 28 [nucl-ex/0410022].
- [3] PHENIX collaboration, K. Adcox et al., *Formation of dense partonic matter in relativistic nucleus nucleus collisions at RHIC: experimental evaluation by the PHENIX collaboration*, *Nucl. Phys. A* **757** (2005) 184 [nucl-ex/0410003].
- [4] STAR collaboration, J. Adams et al., *Experimental and theoretical challenges in the search for the quark gluon plasma: the STAR collaboration's critical assessment of the evidence from RHIC collisions*, *Nucl. Phys. A* **757** (2005) 102 [nucl-ex/0501009].
- [5] P.F. Kolb, P. Huovinen, U.W. Heinz and H. Heiselberg, *Elliptic flow at SPS and RHIC: from kinetic transport to hydrodynamics*, *Phys. Lett. B* **500** (2001) 232 [hep-ph/0012137].
- [6] P. Huovinen, P.F. Kolb, U.W. Heinz, P.V. Ruuskanen and S.A. Voloshin, *Radial and elliptic flow at RHIC: further predictions*, *Phys. Lett. B* **503** (2001) 58 [hep-ph/0101136].
- [7] D. Teaney, J. Lauret and E.V. Shuryak, *Flow at the SPS and RHIC as a quark gluon plasma signature*, *Phys. Rev. Lett.* **86** (2001) 4783 [nucl-th/0011058].
- [8] M. Luzum and P. Romatschke, *Conformal Relativistic Viscous Hydrodynamics: applications to RHIC*, arXiv:0804.4015.
- [9] P. Romatschke and U. Romatschke, *Viscosity information from relativistic nuclear collisions: how perfect is the fluid observed at RHIC?*, *Phys. Rev. Lett.* **99** (2007) 172301 [arXiv:0706.1522].
- [10] K. Dusling and D. Teaney, *Simulating elliptic flow with viscous hydrodynamics*, *Phys. Rev. C* **77** (2008) 034905 [arXiv:0710.5932].
- [11] H. Song and U.W. Heinz, *Suppression of elliptic flow in a minimally viscous quark-gluon plasma*, *Phys. Lett. B* **658** (2008) 279 [arXiv:0709.0742].

- [12] H. Song and U.W. Heinz, *Causal viscous hydrodynamics in 2+1 dimensions for relativistic heavy-ion collisions*, *Phys. Rev. C* **77** (2008) 064901 [[arXiv:0712.3715](#)].
- [13] A.K. Chaudhuri, *Viscous fluid dynamics in Au+Au collisions at RHIC*, [arXiv:0801.3180](#).
- [14] D. Teaney, *Effect of shear viscosity on spectra, elliptic flow and Hanbury Brown-Twiss radii*, *Phys. Rev. C* **68** (2003) 034913 [[nucl-th/0301099](#)].
- [15] L.P. Csernai, J.I. Kapusta and L.D. McLerran, *On the strongly-interacting low-viscosity matter created in relativistic nuclear collisions*, *Phys. Rev. Lett.* **97** (2006) 152303 [[nucl-th/0604032](#)].
- [16] R. Kubo, *Statistical mechanical theory of irreversible processes. 1. General theory and simple applications in magnetic and conduction problems*, *J. Phys. Soc. Jap.* **12** (1957) 570.
- [17] F. Karsch and H.W. Wyld, *Thermal Green's functions and transport coefficients on the lattice*, *Phys. Rev. D* **35** (1987) 2518.
- [18] H.B. Meyer, *Computing the viscosity of the QGP on the lattice*, [arXiv:0805.4567](#).
- [19] RBC collaboration, F. Karsch, *Equation of state and more from lattice regularized QCD*, [arXiv:0804.4148](#).
- [20] P. Arnold, C. Dogan and G.D. Moore, *The bulk viscosity of high-temperature QCD*, *Phys. Rev. D* **74** (2006) 085021 [[hep-ph/0608012](#)].
- [21] P. Arnold, G.D. Moore and L.G. Yaffe, *Transport coefficients in high temperature gauge theories. I: leading-log results*, *JHEP* **11** (2000) 001 [[hep-ph/0010177](#)].
- [22] P. Arnold, G.D. Moore and L.G. Yaffe, *Transport coefficients in high temperature gauge theories. II: beyond leading log*, *JHEP* **05** (2003) 051 [[hep-ph/0302165](#)].
- [23] G.D. Moore and O. Saremi, *Bulk viscosity and spectral functions in QCD*, [arXiv:0805.4201](#).
- [24] G. Aarts and J.M. Martinez Resco, *Transport coefficients, spectral functions and the lattice*, *JHEP* **04** (2002) 053 [[hep-ph/0203177](#)].
- [25] G. Aarts and J.M. Martinez Resco, *Continuum and lattice meson spectral functions at nonzero momentum and high temperature*, *Nucl. Phys. B* **726** (2005) 93 [[hep-lat/0507004](#)].
- [26] H.B. Meyer, *A calculation of the bulk viscosity in SU(3) gluodynamics*, *Phys. Rev. Lett.* **100** (2008) 162001 [[arXiv:0710.3717](#)].
- [27] H.B. Meyer, *A calculation of the shear viscosity in SU(3) gluodynamics*, *Phys. Rev. D* **76** (2007) 101701 [[arXiv:0704.1801](#)].
- [28] A. Nakamura and S. Sakai, *Transport coefficients of gluon plasma*, *Phys. Rev. Lett.* **94** (2005) 072305 [[hep-lat/0406009](#)].
- [29] M. Asakawa and T. Hatsuda, *J/ψ and η/c in the deconfined plasma from lattice QCD*, *Phys. Rev. Lett.* **92** (2004) 012001 [[hep-lat/0308034](#)].
- [30] G. Aarts et al., *Charmonium spectral functions in two-flavour QCD*, *Nucl. Phys. A* **785** (2007) 198 [[hep-lat/0608009](#)].
- [31] G. Aarts, C. Allton, M.B. Oktay, M. Peardon and J.-I. Skullerud, *Charmonium at high temperature in two-flavor QCD*, *Phys. Rev. D* **76** (2007) 094513 [[arXiv:0705.2198](#)].

- [32] G. Aarts, C. Allton, J. Foley, S. Hands and S. Kim, *Spectral functions at small energies and the electrical conductivity in hot, quenched lattice QCD*, *Phys. Rev. Lett.* **99** (2007) 022002 [[hep-lat/0703008](#)].
- [33] E. Braaten and R.D. Pisarski, *Soft amplitudes in hot gauge theories: a general analysis*, *Nucl. Phys.* **B 337** (1990) 569.
- [34] H.B. Meyer, *Finite temperature sum rules in lattice gauge theory*, *Nucl. Phys.* **B 795** (2008) 230 [[arXiv:0711.0738](#)].
- [35] D. Teaney, *Finite temperature spectral densities of momentum and R-charge correlators in $N = 4$ Yang-Mills theory*, *Phys. Rev.* **D 74** (2006) 045025 [[hep-ph/0602044](#)].
- [36] D.T. Son and A.O. Starinets, *Viscosity, black holes and quantum field theory*, *Ann. Rev. Nucl. Part. Sci.* **57** (2007) 95 [[arXiv:0704.0240](#)].
- [37] S. Sakai and A. Nakamura, *Lattice calculation of the QGP viscosities - Present results and next project -*, *PoS(LATTICE 2007)*221 [[arXiv:0710.3625](#)].
- [38] H.B. Meyer, *Locality and statistical error reduction on correlation functions*, *JHEP* **01** (2003) 048 [[hep-lat/0209145](#)].
- [39] H.B. Meyer, *The Yang-Mills spectrum from a 2-level algorithm*, *JHEP* **01** (2004) 030 [[hep-lat/0312034](#)].
- [40] P. Majumdar, Y. Koma and M. Koma, *Glueball masses in 4D U(1) lattice gauge theory using the multi-level algorithm*, *Nucl. Phys.* **B 677** (2004) 273 [[hep-lat/0309003](#)].
- [41] G. Aarts, C. Allton, J. Foley, S. Hands and S. Kim, *Meson spectral functions at nonzero momentum in hot QCD*, *Nucl. Phys.* **A 785** (2007) 202 [[hep-lat/0607012](#)].